Am J Transl Res 2017;9(7):3433-3442
www.ajtr.org /ISSN:1943-8141/AJTR0055499

Original Article

MicroRNA-1907 enhances atherosclerosis-associated endothelial cell apoptosis by suppressing Bcl-2

Jin Zhao[1], Shu-Lin Ou[2], Wei-You Wang[3], Chang Yan[2], Lu-Xiang Chi[2]

[1]Center of Translational Medicine, College of Pharmacy, Third Military Medical University, Chongqing 400038, China; [2]Department of Cardiology, Southwest Hospital, Third Military Medical University, Chongqing 400038, China; [3]Third Department of Internal Medicine, Chongqing Thirteenth People's Hospital, Chongqing 400053, China

Received February 26, 2017; Accepted May 20, 2017; Epub July 15, 2017; Published July 30, 2017

Abstract: Injury and endothelial cell apoptosis are hall marks of atherosclerosis (AS). However, the mechanisms underlying its pathogenesis remain ill-defined. Recent evidence of a role for microRNAs in AS-associated endothelial cell apoptosis encouraged us to address this question. Here, AS was developed in ApoE (-/-) mice supplied with a high-fat diet (HFD), compared to ApoE (-/-) mice supplied with a normal diet (ND). Mouse endothelial cells were isolated from the aortic arch using flow cytometry based on their expression of CD31. Human aortic endothelial cells (HAECs) were treated with oxidized low-density lipoprotein (ox-LDL) as an *in vitro* model for AS. Gene expression was quantified by RT-qPCR and protein levels were analyzed by Western blotting. Apoptosis was evaluated by FITC Annexin V Apoptosis assay and by TUNEL staining. Predicting binding patterns between miRNAs and the 3'-UTR of mRNA from the target gene was performed by bioinformatics analyses and confirmed by a dual luciferase reporter assay. We found that HFD mice, but not ND mice, developed AS in 12 weeks. A significant reduction in endothelial cells and a significant increase in mesenchymal cells were detected in the aortic arch of the HFD mice, compared to those of ND mice. Endothelial cell apoptosis was significantly higher in HFD mice, seemingly due to functional suppression of protein translation of anti-apoptotic Bcl-2 protein through upregulation of miR-1907, confirmed by *in vitro* analysis. Moreover, inhibition of miR-1907 abolished the effects of ox-LDL-induced apoptotic cell death on HAECs. Thus, AS-associated endothelial cell apoptosis may partially result from downregulation of Bcl-2, via upregulation of miR-1907 which binds and suppresses the translation of Bcl-2 mRNA.

Keywords: Atherosclerosis, endothelial cell apoptosis, ApoE (-/-), high fat diet (HFD), ox-LDL, Bcl-2, miR-1907

Introduction

Atherosclerosis (AS) is a leading health issue among people of advanced age worldwide [1, 2]. Endothelial cell injury and apoptosis play an essential role in the development and pathogenesis of AS [3-7]. However, the molecular mechanisms underlying endothelial cell apoptosis are poorly understood.

Apolipoprotein E (ApoE) is well-known to be a potent suppressor of AS [8, 9]. ApoE-deficient (ApoE -/-) mice display enhanced chronic inflammatory responses to diet-induced hypercholesterolemia [8, 9]. Therefore, providing 12-weeks of a high fat diet (HFD) in (ApoE -/-) mice has been used as an AS model for years [10-12].

MicroRNAs (miRNAs) are small non-coding RNAs that post-transcriptionally control protein translation through pairing with the 3'-untranslated region (3'-UTR) of the mRNA from their target genes. Recently, miRNAs have been found to regulate the development of AS via a variety of target factors or pathways [13]. Specifically, systemic delivery of miR-181b has been shown to attenuate AS through modulation of NF-κB signaling in endothelial cells [14]. Moreover, inhibition of miR-92a was found to prevent endothelial dysfunction and development of AS in mice [15]. In addition, MiR-126-5p was defined as a mitotic factor for endothelial cell growth and overexpression of miR-126-5p inhibited AS by suppressing Dlk1 [16]. Furthermore, miR-26a was revealed to be an anti-apoptotic miRNA which prevents endothelial cell apoptosis by targeting TRPC6 in the setting of AS [17]. These studies encouraged us to investigate the role of miRNAs in AS-associated endothelial cell apoptosis in the current study.

Here, AS was developed in ApoE (-/-) mice supplied with HFD, compared to ApoE (-/-) mice supplied with a normal diet (ND). Mouse endothelial cells were isolated from the aortic arch using flow cytometry based on their expression of CD31. Oxidized low-density lipoprotein (ox-LDL) was used to treat human aortic endothelial cells (HAECs) as an *in vitro* model for AS. Gene expression was quantified by RT-qPCR and protein levels were analyzed by Western blotting. Apoptosis was evaluated by FITC Annexin V Apoptosis essay and by TUNEL staining. Prediction of the binding between miRNAs and the 3'-UTR of mRNA from the target gene was performed by bioinformatics analyses and confirmed by a dual luciferase reporter assay. We found that HFD mice, but not ND mice, developed AS in 12 weeks. Significantly reduced endothelial cell markers and significantly increased mesenchymal cell markers were detected in the aortic arch of the HFD mice, compared to ND mice. Endothelial cell apoptosis was significantly higher in HFD mice, seemingly due to functional suppression of protein translation of anti-apoptotic Bcl-2 protein via upregulation of miR-1907. Similar results were obtained from *in vitro* analysis. Inhibition of miR-1907 abolished the effects of ox-LDL-induced apoptotic cell death on HAECs. Thus, we conclude that AS-associated endothelial cell apoptosis may partially result from down-regulation of Bcl-2, via upregulation of miR-1907 that binds and suppresses translation of Bcl-2 mRNA.

Materials and methods

Ethics statement

This study was approved by the Animal Care and Use Committee of Third Military Medical University. All experimental procedures were performed in accordance with the Guide for the Care and Use of Laboratory Animals, published by the US National Institutes of Health. All experiments were conducted under the supervision of the facility's Institutional Animal Care and Use Committee according to an Institutional Animal Care and Use Committee-approved protocol.

Animal models

ApoE-/- mice at 8 weeks of age were purchased from Jackson Laboratory (Bar Harbor, ME, USA) or bred in-house and maintained under sterile conditions. The animals were randomly divided into two groups: the normal-diet group (ND) and the high-fatdiet (HFD) group. The animals of the HFD group were maintained for 12 weeks to induce AS.

Quantification of atherosclerotic lesions

Mouse aortic arch was excised and fixed with 4% paraformaldehyde for 6 hours, cryo-protected in 30% sucrose for 24 hours, OCT-embedded, and sectioned at 6 μm thickness. AS lesions were examined by H&E staining and Oil red O staining (Oil red O staining kit, Abcam, Cambridge, MA, USA). The data were calculated from 10 mice from each group.

Cell culture and transfection

Human aortic endothelial cells (HAECs, American Type Culture Collection, Rockville, MD, USA) were cultured in Endothelial Cell Medium supplemented with endothelial cell growth factors, 5% fetal bovine serum (FBS, Invitrogen, CA, Carlsbad, USA) and 1% penicillin/streptomycin (Invitrogen) at 37°C with 5% CO_2. HAECs were transiently transfected with miR-1907 mimics, antisense for miR-1907 (as-miR-1907) or null controls (RiboBio Co., Ltd., Guangzhou, Guangdong, China), using Lipofectamine 2000 reagent (Invitrogen). The transfection efficiency was nearly 100%.

Ox-LDL treatment of cells

One day after cell transfection, the HAECs were treated with or without 100 μg/ml oxidized low-density lipoprotein (ox-LDL, Beijing Xiesheng Bio-Technology Limited, Beijing, China), after which the cells underwent flow cytometry or protein/RNA extraction.

Cell viability by cell counting kit-8 (CCK-8) assay

The CCK-8 detection kit (Sigma-Aldrich, St. Louis, MO, USA) was used to measure cell viability according to the manufacturer's instructions.

Apoptosis assay and flow cytometry

The dissociated tissue or cultured cells were re-suspended at a density of 10^6 cells/ml in PBS. After double staining with FITC-Annexin V and propidium iodide (PI) from a FITC Annexin V Apoptosis Detection Kit I (Becton-Dickinson Biosciences, San Jose, CA, USA), cells were

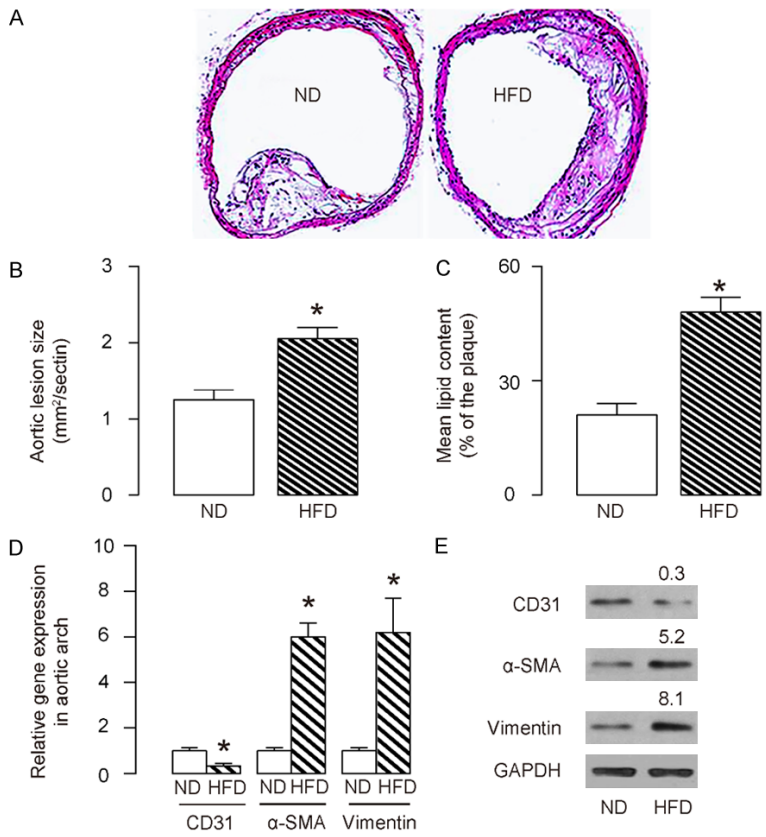

Figure 1. AS is developed in HFD mice. ApoE (-/-) mice were treated with high-fat diet (HFD) or normal diet (ND) as a control. (A-C) After 12 weeks, H&E-staining on aortic sinus showed a significant increase in aortic lesion size, shown by representative images (A), and by quantification (B). (C) Quantification of lipid content by Oil-red-O-staining on aortic sinus. (D, E) The aortic arch was isolated for analyzing the levels of CD31, α-SMA and Vimentin by RT-qPCR (D), and by Western blotting. *P < 0.05. N=10.

analyzed using FACScan flow cytometer (Becton-Dickinson Biosciences) for determination of Annexin V+ PI- apoptotic cells. For analyses and isolation of CD31+ cells, the dissociated tissue cells were incubated with PE-cy7-CD31 (Becton-Dickinson Biosciences).

TUNEL staining

TUNEL staining was performed using a TUNEL fluorescence FITC kit (Roche, Indianapolis, IN, USA). HAECs were fixed with 4% paraformaldehyde followed by permeabilization with 0.1% Triton X-100. Then, cells were incubated with TUNEL reaction mixture at 37°C for 1 h, after which the stained tissues and cells were examined.

RT-qPCR

Total RNA was isolated from mouse aortic arch, sorted cells or cultured cells with miRN easy mini kit (Qiagen, Hilden, Germany). The extracted RNA was reverse transcribed into cDNA using a High-Capacity cDNA Reverse Transcription Kit (Applied Biosystems, Foster City, CA, USA). The first-strand cDNA was used for real-time PCR to quantify mRNA expressions using QuantiTect SYBR Green PCR Kit (Qiagen). All primers were purchased from Qiagen. Data were collected and analyzed using 2-ΔΔCt method for quantification of the relative mRNA expression levels. Values of genes were first normalized against GAPDH, and then compared to the experimental controls.

Western blotting

The cells were lysed with RIPA buffer containing protease and phosphatase inhibitors (complete ULTRA Tablets, Roche, Nutley, NJ, USA). After centrifugation, the supernatant was collected and quantified. The proteins were then separated by SDS-PAGE and transferred to nitrocellulose membranes. After blocking with 5% non-fat milk, the membranes were probed withrat-anti-CD31 (Becton-Dickinson Biosciences, San Jose, CA, USA), rabbit-anti-alpha smooth muscle actin (α-SMA), rabbit anti-Vimentin, rabbit-anti-Bcl-2, rabbit-anti-Bcl-2, rabbit-anti-BAD, rabbit-anti-BAX rabbit-anti-BID and rabbit-anti-GAPDH (all from Cell Signaling Technology, Danvers, MA, USA). Secondary antibodies were HRP-conjugated against rat or rabbit (Jackson ImmunoResearch Labs, West Grove, PA, USA). The protein levels were first normalized to GAPDH, and then normalized to the experimental controls. Densitometry of Western blots was quantified with NIH ImageJ software.

MiRNA target prediction and 3'-UTR luciferase-reporter assay

MiRNAs targets were predicted using the algorithms TargetSan. The Bcl-2 3'-UTR wild-type (wt) reporter and mutate (mut) reporter plas-

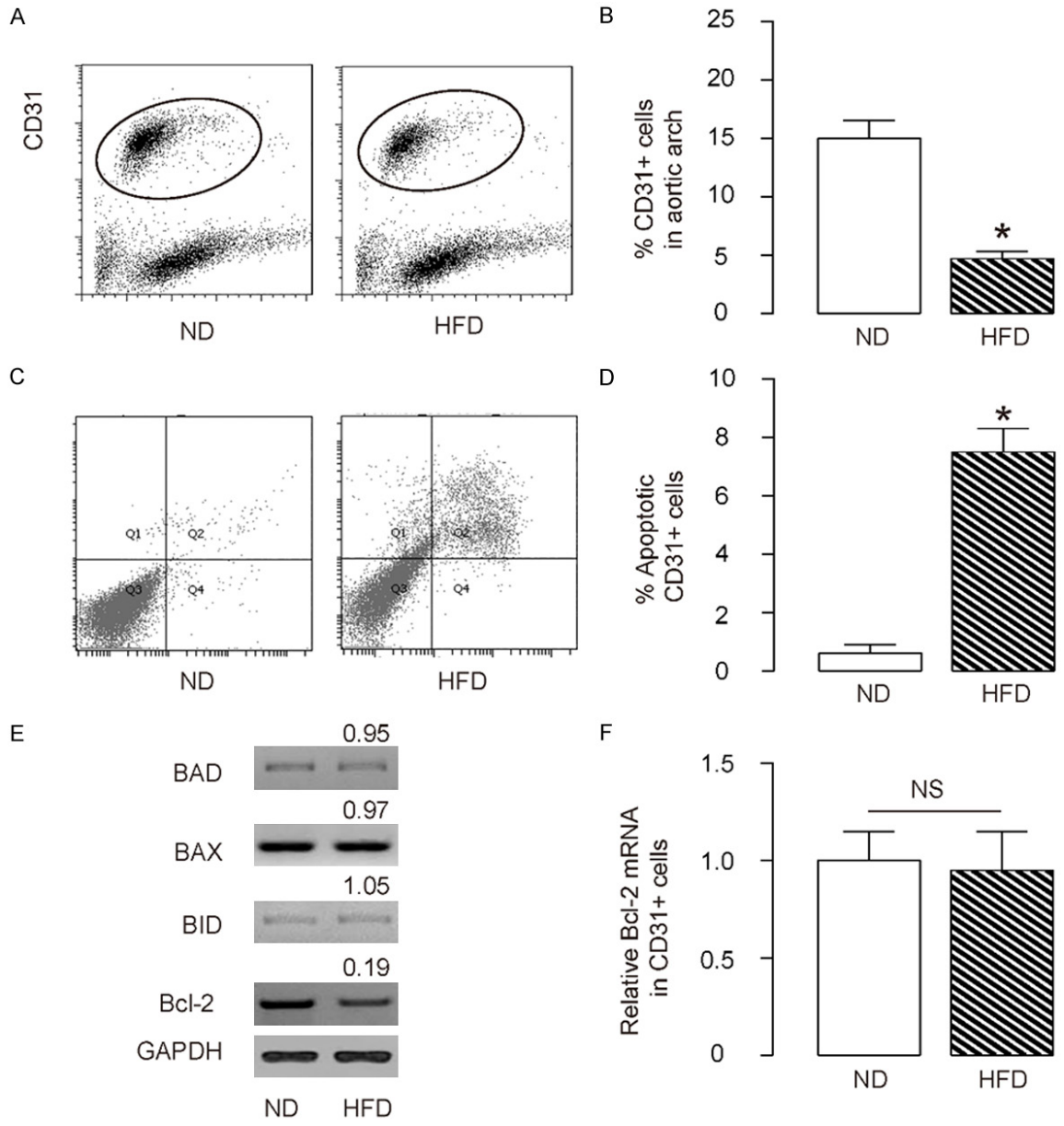

Figure 2. Increased endothelial cell apoptosis occurs in HFD mice. (A, B) CD31+ cells were isolated from dissociated mouse aortic arch by flow cytometry, shown by representative flow charts (A), and by quantification (B). (C, D) The apoptosis of isolated CD31+ cells were analyzed by FITC Annexin V Apoptosis assay, shown by representative flow charts (C), and by quantification (D). (E) Western blotting for apoptosis-associated proteins in purified endothelial cells. (F) RT-qPCR for Bcl-2 in purified endothelial cells.
*P < 0.05. N=10.

mids were purchased from Creative Biogene (Shirley, NY, USA). Co-transfection of HAECs with miR-1907-modification plasmids and Bcl-2 3'-UTR reporter plasmids were performed using Lipofectamine 2000. Cells were collected 48 hours after transfection for assay using the dual-luciferase reporter assay system gene assay kit (Promega, Madison, WI, USA), according to the manufacturer's instructions.

Statistical analyses

The data in this study are shown as the mean ± S.D. Differences among groups were analyzed using one-away ANOVA with a Bonferroni correction, followed by Fisher' Exact Test for comparison of two groups (GraphPad Prism, GraphPad Software, Inc. La Jolla, CA, USA). P < 0.05 was considered significant.

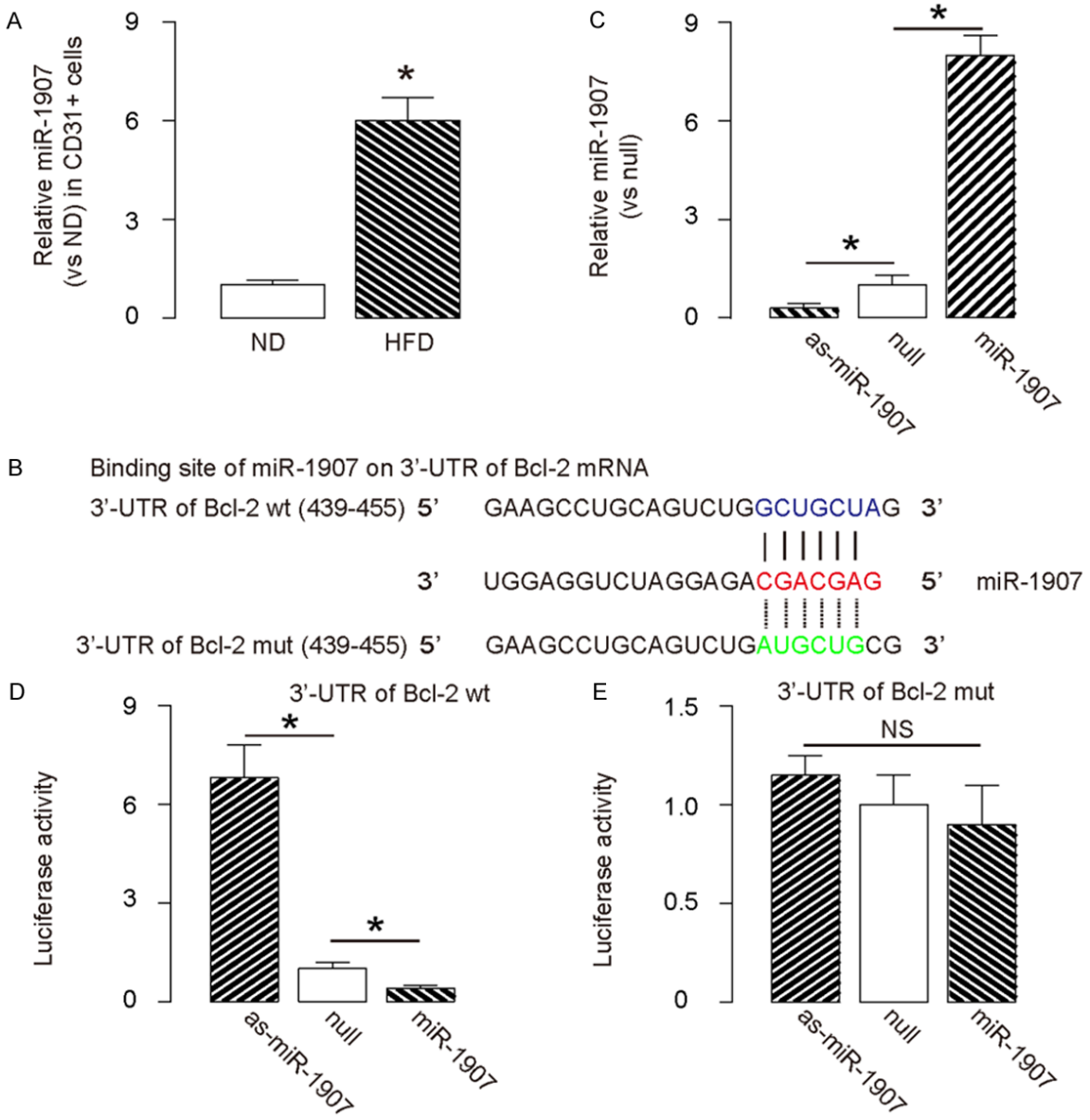

Figure 3. HFD-induced upregulation of miR-1907 suppresses protein translation of Bcl-2. A. RT-qPCR formiR-1907 in CD31+ endothelial cells from HFD or ND mice. B. Bioinformatics analyses showing the binding site of miR-1907 on the wild type (wt) of 3'-UTR of Bcl-2 mRNA as well as the sequence of the mutate (mut) 3'-UTR of Bcl-2 mRNA. C. RT-qPCR levels for miR-1907 in miR-1907-modified human aortic endothelial cells (HAECs), prepared by transfection of the cells with miR-1907 mimics, antisense for miR-1907 (as-miR-1907) or null controls (null). D. Luciferase activity of the wt 3'-UTR of Bcl-2 mRNA by co-transfection of miR-1907-modified plasmids on HAECs. E. Luciferase activity of the mut 3'-UTR of Bcl-2 mRNA by co-transfection of miR-1907-modified plasmids on HAECs. *P < 0.05. NS: non-significant. N=5.

Result

AS is developed in HFD mice

ApoE (-/-) mice were treated with either HFD or ND for 12 weeks, after which the AS lesions were analyzed. H&E-stained aortic sinus displayed a significant increase in aortic lesion size in HFD mice, compared to ND mice (**Figure 1A**, **1B**). Moreover, Oil-red-O-stained aortic sinus displayed a significant increase in lipid content (**Figure 1C**). These data suggest that HFD successfully induced ASin ApoE (-/-) mice, confirming the establishment of the model. The aortic arch was then isolated for analysis of the levels of endothelial marker CD31 and the mesenchymal markers α-SMA and Vimentin. We

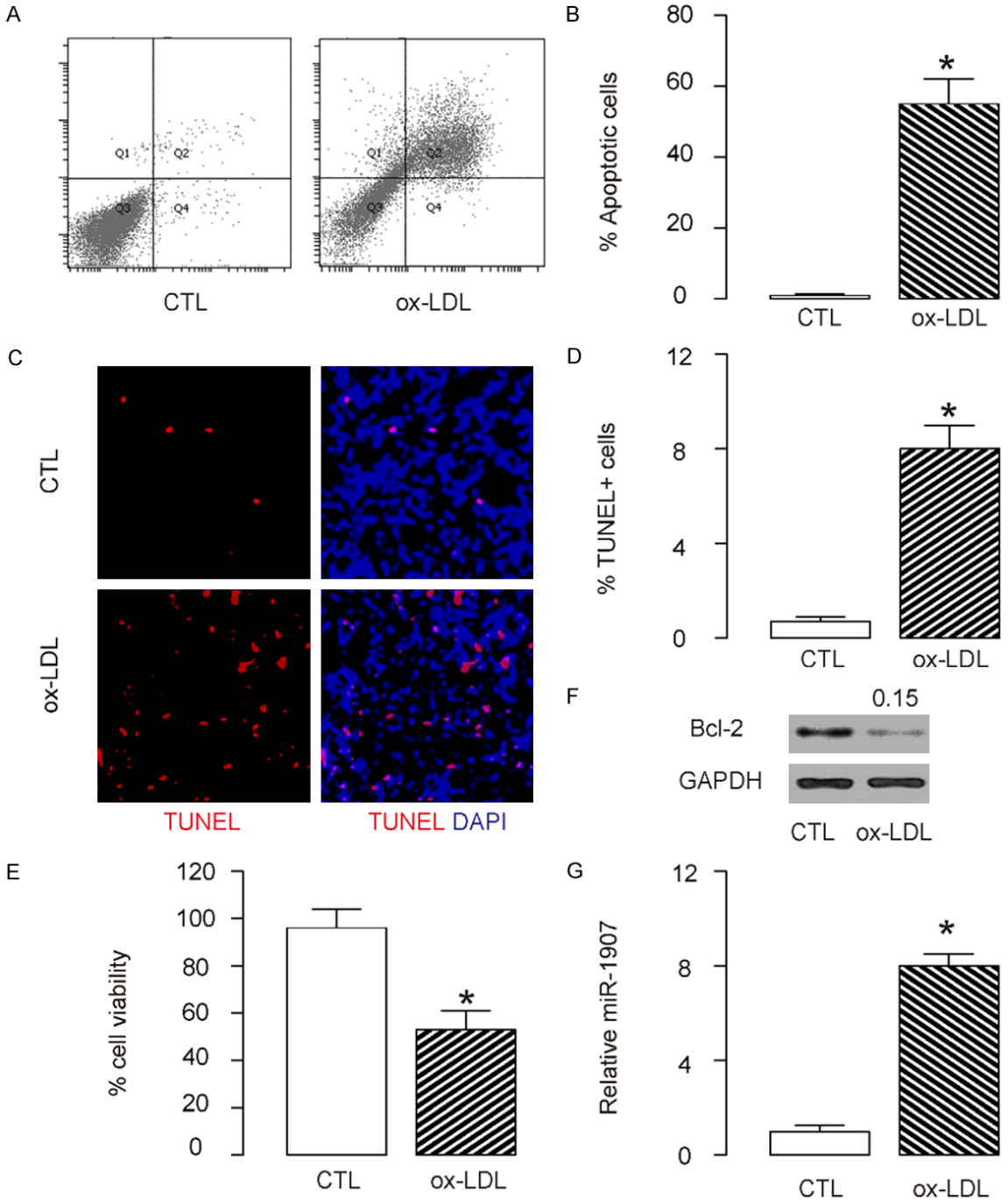

Figure 4. Ox-LDL-treated HAECs recapitulate the findings in HFD mice. HAECs were treated with or without 100 μg/ml ox-LDL to induce cell apoptosis. (A, B) Analyses of cell apoptosis by FITC Annexin V Apoptosis assay, shown by representative flow charts (A), and by quantification (B). (C, D) Analyses of cell apoptosis by TUNEL assay, shown by representative images (C), and by quantification (D). (E) Quantification of viable cell number in a CCK-8 assay. (F) Western blotting for Bcl-2. (G) RT-qPCR for miR-1907. *P < 0.05. N=5.

detected significantly lower levels of CD31 by mRNA (**Figure 1D**), and by Western blot (**Figure 1E**) in aortic arch from HFD mice, compared to ND mice. Moreover, we detected significantly higher levels of α-SMA and Vimentin by mRNA (**Figure 1D**), and by Western blot (**Figure 1E**). Together, these data suggest that HFD induces AS in ApoE (-/-) mice.

Increased endothelial cell apoptosis occurs in HFD mice

To specifically study endothelial cells in the aortic arch, we isolated CD31+ cells from the dissociated mouse aortic arch by flow cytometry (**Figure 2A**). We found that the percentage of CD31+ endothelial cells in the aortic arch from HFD mice was significantly lower than that in ND mice (**Figure 2B**), suggesting that the low CD31 levels in the aorta of HFD mice may result from reduced endothelial cells. In order to understand the mechanism, the isolated CD31+ cells were further subjected to FITC Annexin V Apoptosis essay. We detected a significantly higher percentage of apoptotic CD31+ endothelial cells in HFD mice, compared to ND mice, shown by representative flow charts (**Figure 2C**), and by quantification (**Figure 2D**). Thus, HFD induces endothelial cell apoptosis in ApoE (-/-) mice. To figure out the apoptotic factors that may be involved, we examined the major candidates BAD, Bax, Bid and Bcl-2. Although pro-apoptotic proteins were not significantly altered, we detected significantly lower levels of anti-apoptotic proteins Bcl-2 in endothelial cells from HFD mice, compared to ND mice (**Figure 2E**). Thus, we focused on Bcl-2 in the current study. To our surprise, mRNA levels of Bcl-2, unlike the protein levels, were not significantly altered in endothelial cells from HFD mice, compared to ND mice (**Figure 2F**), suggesting that the alteration of Bcl-2 protein levels may be due to post-transcriptional regulation, such as by miRNAs.

HFD-induced upregulation of miR-1907 suppresses protein translation of Bcl-2

Next, we examined the underlying mechanisms. All Bcl-2-targeting miRNAs were then determined by bioinformatics analyses, from which we found that miR-1907 levels were significantly increased in CD31+ endothelial cells in HFD mice (**Figure 3A**). MiR-1907 targets the 3'-UTR of Bcl-2 mRNA at one binding site (**Figure 3B**). MiR-1907 mimics, antisense for miR-1907 (as-miR-1907) and null controls (null) were then prepared to transfect human aortic endothelial cells (HAECs) to confirm the potential of modification of miR-1907 levels by these plasmids (**Figure 3C**). Next, luciferase reporters containing the 3'-UTR of Bcl-2 or a mutated 3'-UTR of Bcl-2 in the miR-1907 binding site were constructed and transfected into HAECs (**Figure 3B**). We found that miR-1907 markedly inhibited the luciferase activity of the vector containing the wild-type binding site, whereas the as-miR-1907 increased luciferase activity (**Figure 3D**). Moreover, transfection of miR-1907 or as-miR-1907 did not affect the luciferase activity of the reporter carrying the mutated miR-1907 binding site (**Figure 3E**). Together, these data suggest that HFD-induced upregulation of miR-1907 may suppress protein translation of Bcl-2.

Ox-LDL-treated HAECs upregulate miR-1907 and increase apoptosis

HAECs were treated with 100 μg/ml oxidized low-density lipoprotein (ox-LDL) as an *in vitro* model to study endothelial cells in the setting of AS. First, we confirmed that ox-LDL significantly increased cell apoptosis, by FITC Annexin V Apoptosis essay (**Figure 4A**, **4B**), and by TUNEL assay (**Figure 4C**, **4D**). Moreover, endothelial cell apoptosis resulted in a significant reduction in viable cell number in a CCK-8 assay (**Figure 4E**). Furthermore, ox-LDL significantly decreased Bcl-2 protein levels (**Figure 4F**), and significantly increased miR-1907 levels (**Figure 4G**).

Depletion of miR-1907 reduces ox-LDL-induced apoptotic death of HAECs

Finally, we examined whether depletion of miR-1907 may inhibit or attenuate the apoptotic cell death of HAECs by ox-LDL. HAECs were thus transfected with null or as-miR-1907, and then exposed to ox-LDL. We found that depletion of miR-1907 significantly decreased ox-LDL-induced cell apoptosis, by FITC Annexin V Apoptosis essay (**Figure 5A**, **5B**), and by TUNEL assay (**Figure 5C**, **5D**), resulting in increases in viable endothelial cell number by ox-LDL treatment in a CCK-8 assay (**Figure 5E**), seemingly through increases inBcl-2 protein (**Figure 5F**). Thus, depletion of miR-1907 reduces ox-LDL-induced apoptotic death of HAECs.

Discussion

During vascular homeostasis, the endothelium helps to mediate vasodilation, suppression of smooth muscle cell outgrowth, and inhibition of aberrant inflammatory responses [3-7]. Ample evidence has highlighted endothelial dysfunction as an early characteristic of AS, since there is endothelial cell dysfunction and injury before

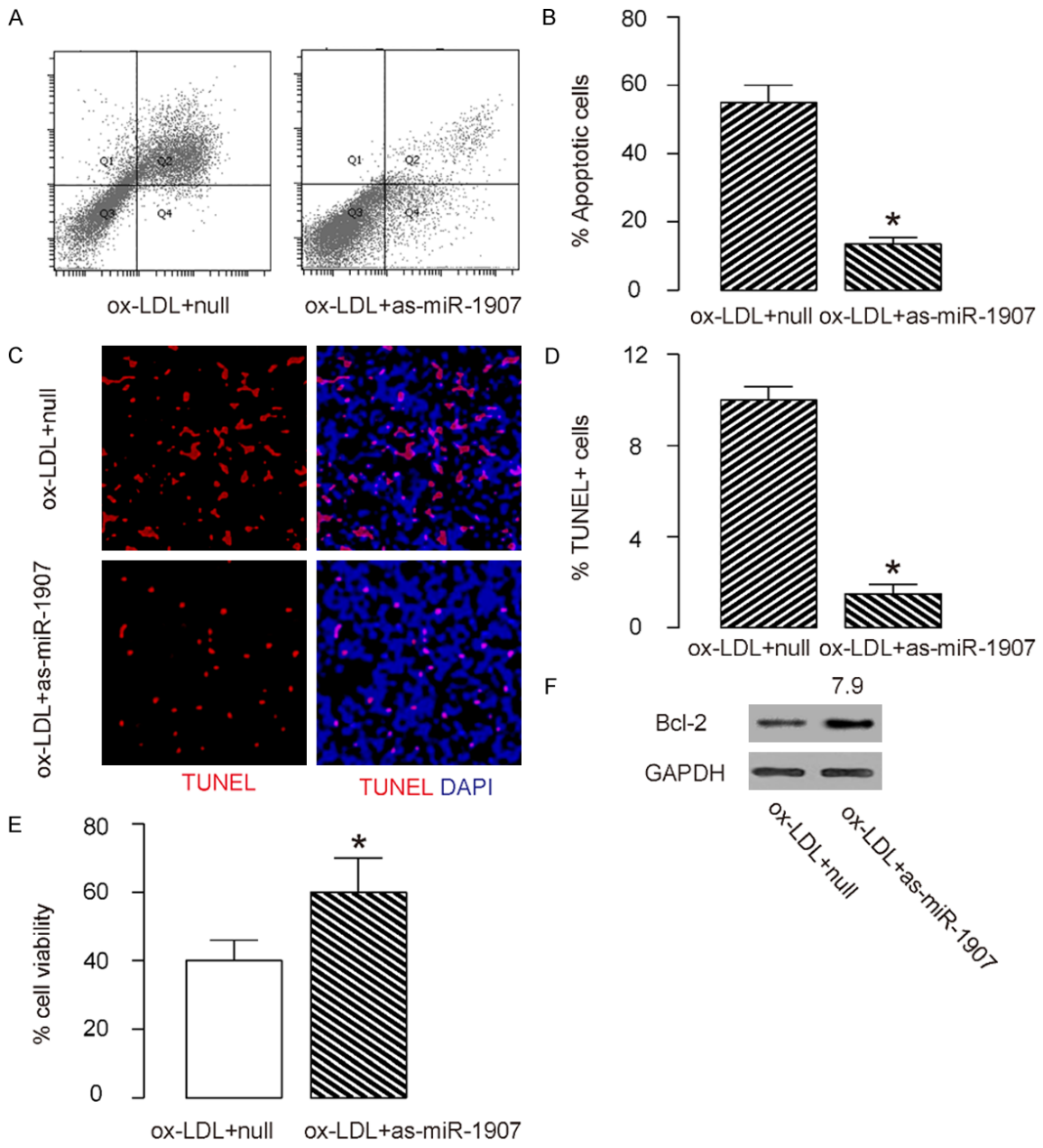

Figure 5. Depletion of miR-1907 reduces ox-LDL-induced apoptotic death of HAECs. HAECs were first transfected with null or as-miR-1907 plasmids, and then treated with or without 100 μg/ml ox-LDL to induce cell apoptosis. (A, B) Analyses of cell apoptosis by FITC Annexin V Apoptosis assay, shown by representative flow charts (A), and by quantification (B). (C, D) Analyses of cell apoptosis by TUNEL assay, shown by representative images (C), and by quantification (D). (E) Quantification of viable cell number in a CCK-8 assay. (F) Western blotting for Bcl-2. *$P < 0.05$. N=5.

the onset of structural alterations to the vessel wall [3-7]. On the other hand, many risk factors predisposing to AS have been demonstrated to induce endothelial dysfunction, including upregulation of nitric oxide production or activity, as well as reduction of oxidative stress [3-7].

Mechanistically, interactions among endothelial cells and other cell types like T lymphocytes, macrophages and smooth muscle cells coordinate the pathogenesis of AS. It is likely that proatherosclerotic factors are produced and secreted to induce endothelial cell apoptosis

[3-7]. However, the detailed molecular signaling remains ill-defined.

Aberrantly expressed miRNAs have recently been reported to play a role in the regulation of endothelial cell survival/death in the setting of AS. For example, miR-26a was revealed to be an anti-apoptotic miRNA which prevents endothelial cell apoptosis in the development of AS [17]. In this study, the authors ascertained that miR-26a is a novel anti-apoptotic miRNA which directly targets TRPC6 in vascular endothelial cells, but is dysregulated in AS. AS-related endothelial cell apoptosis is regulated in a pathway involving miR-26a, TRPC6, intracellular calcium, cytochrome c and caspase 3 [17]. Moreover, AS-associated endothelial cell apoptosis has also been attributed to the down-regulation of Bcl-2, through increased miR-429 that binds to and suppresses the translation of Bcl-2 mRNA [18]. However, targets other than TRPC6 and Bcl-2 that are associated with AS-related endothelial cell apoptosis have not been reported.

Here, we found that ApoE (-/-) mice treated with 12 weeks of HFD developed AS, while the control ApoE (-/-) mice fed with ND did not. HFD mice displayed typical features of AS. When we analyzed major apoptosis-associated proteins by Western blot in CD31+ endothelial cells from those mice, we found that Bcl-2 was suppressed in CD31+ endothelial cells from HFD mice.

Since the mRNA levels of Bcl-2 appeared unchanged, we proposed that Bcl-2 might be regulated by a miRNA. All Bcl-2-targeting miRNAs were then determined by bioinformatics analyses, and we screened all these miRNAs and found that miR-1907 levels were significantly increased in CD31+ endothelial cells from HFD mice. We thus performed an *in vitro* analysis on the role of miR-1907 in an experimental model of AS, and confirmed this regulation loop in the control of AS-associated endothelial cell apoptosis by a loss-of-function approach. MiR-1907 is a miRNA, the function of which is poorly understood. First, haplo insufficiency of the gene appears to be associated with craniofacial abnormalities [19]. Moreover, elevated expression of circulating miR-1907 has been shown to be a specific response to severe EV71 infections [20]. Our study should provide additional insight into the biological function of miR-1907.

In summary, our study identified a new role for miR-1907 in the regulation of endothelial cell apoptosis during AS, and sheds new light that may facilitate the development of innovative AS therapies.

Acknowledgements

This work was supported by internal funding of Third Military Medical University.

Disclosure of conflict of interest

None.

Address correspondence to: Lu-Xiang Chi, Department of Cardiology, Southwest Hospital, Third Military Medical University, 30 Gaotanyan, Chongqing 400038, China. Tel: +862368754118; E-mail: zjin807@yeah.net; chi68754271@126.com

References

[1] Schmitz G and Grandl M. Lipid homeostasis in macrophages-implications for atherosclerosis. Rev Physiol Biochem Pharmacol 2008; 160: 93-125.

[2] Liehn EA, Zernecke A, Postea O and Weber C. Chemokines: inflammatory mediators of atherosclerosis. Arch Physiol Biochem 2006; 112: 229-238.

[3] Peng N, Meng N, Wang S, Zhao F, Zhao J, Su L, Zhang S, Zhang Y, Zhao B and Miao J. An activator of mTOR inhibits oxLDL-induced autophagy and apoptosis in vascular endothelial cells and restricts atherosclerosis in apolipoprotein E(-)/(-) mice. Sci Rep 2014; 4: 5519.

[4] Sun C, Wu MH and Yuan SY. Nonmuscle myosin light-chain kinase deficiency attenuates atherosclerosis in apolipoprotein E-deficient mice via reduced endothelial barrier dysfunction and monocyte migration. Circulation 2011; 124: 48-57.

[5] Leppanen P, Koota S, Kholova I, Koponen J, Fieber C, Eriksson U, Alitalo K and Yla-Herttuala S. Gene transfers of vascular endothelial growth factor-A, vascular endothelial growth factor-B, vascular endothelial growth factor-C, and vascular endothelial growth factor-D have no effects on atherosclerosis in hypercholesterolemic low-density lipoprotein-receptor/apolipoprotein B48-deficient mice. Circulation 2005; 112: 1347-1352.

[6] Foteinos G, Afzal AR, Mandal K, Jahangiri M and Xu Q. Anti-heat shock protein 60 autoantibodies induce atherosclerosis in apolipoprotein E-deficient mice via endothelial damage. Circulation 2005; 112: 1206-1213.

[7] Barton M, Haudenschild CC, d'Uscio LV, Shaw S, Munter K and Luscher TF. Endothelin ETA receptor blockade restores NO-mediated endothelial function and inhibits atherosclerosis in apolipoprotein E-deficient mice. Proc Natl Acad Sci U S A 1998; 95: 14367-14372.

[8] Zhi K, Li M, Zhang X, Gao Z, Bai J, Wu Y, Zhou S, Li M and Qu L. alpha4beta7 Integrin (LPAM-1) is upregulated at atherosclerotic lesions and is involved in atherosclerosis progression. Cell Physiol Biochem 2014; 33: 1876-1887.

[9] Dou L, Lu Y, Shen T, Huang X, Man Y, Wang S and Li J. Panax notogingseng saponins suppress RAGE/MAPK signaling and NF-kappaB activation in apolipoprotein-E-deficient atherosclerosis-prone mice. Cell Physiol Biochem 2012; 29: 875-882.

[10] Watson AM, Li J, Samijono D, Bierhaus A, Thomas MC, Jandeleit-Dahm KA and Cooper ME. Quinapril treatment abolishes diabetes-associated atherosclerosis in RAGE/apolipoprotein E double knockout mice. Atherosclerosis 2014; 235: 444-448.

[11] Chatterjee S, Bedja D, Mishra S, Amuzie C, Avolio A, Kass DA, Berkowitz D and Renehan M. Inhibition of glycosphingolipid synthesis ameliorates atherosclerosis and arterial stiffness in apolipoprotein E-/- mice and rabbits fed a high-fat and -cholesterol diet. Circulation 2014; 129: 2403-2413.

[12] Cavigiolio G and Jayaraman S. Proteolysis of apolipoprotein A-I by secretory phospholipase A(2): a new link between inflammation and atherosclerosis. J Biol Chem 2014; 289: 10011-10023.

[13] Menghini R, Stohr R and Federici M. MicroRNAs in vascular aging and atherosclerosis. Ageing Res Rev 2014; 17: 68-78.

[14] Sun X, He S, Wara AK, Icli B, Shvartz E, Tesmenitsky Y, Belkin N, Li D, Blackwell TS, Sukhova GK, Croce K and Feinberg MW. Systemic delivery of microRNA-181b inhibits nuclear factor-kappaB activation, vascular inflammation, and atherosclerosis in apolipoprotein E-deficient mice. Circ Res 2014; 114: 32-40.

[15] Loyer X, Potteaux S, Vion AC, Guerin CL, Boulkroun S, Rautou PE, Ramkhelawon B, Esposito B, Dalloz M, Paul JL, Julia P, Maccario J, Boulanger CM, Mallat Z and Tedgui A. Inhibition of microRNA-92a prevents endothelial dysfunction and atherosclerosis in mice. Circ Res 2014; 114: 434-443.

[16] Schober A, Nazari-Jahantigh M, Wei Y, Bidzhekov K, Gremse F, Grommes J, Megens RT, Heyll K, Noels H, Hristov M, Wang S, Kiessling F, Olson EN and Weber C. MicroRNA-126-5p promotes endothelial proliferation and limits atherosclerosis by suppressing Dlk1. Nat Med 2014; 20: 368-376.

[17] Zhang Y, Qin W, Zhang L, Wu X, Du N, Hu Y, Li X, Shen N, Xiao D, Zhang H, Li Z, Zhang Y, Yang H, Gao F, Du Z, Xu C and Yang B. MicroRNA-26a prevents endothelial cell apoptosis by directly targeting TRPC6 in the setting of atherosclerosis. Sci Rep 2015; 5: 9401.

[18] Zhang T, Tian F, Wang J, Jing J, Zhou SS and Chen YD. Atherosclerosis-associated endothelial cell apoptosis by miR-429-mediated down regulation of Bcl-2. Cell Physiol Biochem 2015; 37: 1421-1430.

[19] Koufaris C, Papagregoriou G, Kousoulidou L, Moutafi M, Tauber M, Jouret B, Kieffer I, Deltas C, Tanteles GA, Anastasiadou V, Patsalis PC and Sismani C. Haploinsufficiency of the miR-873/miR-876 microRNA cluster is associated with craniofacial abnormalities. Gene 2015; 561: 95-100.

[20] Wang RY, Weng KF, Huang YC and Chen CJ. Elevated expression of circulating miR876-5p is a specific response to severe EV71 infections. Sci Rep 2016; 6: 24149.